International Journal of Heat and Fluid Flow 30 (2009) 66–75

Contents lists available at ScienceDirect

International Journal of Heat and Fluid Flow

journal homepage: www.elsevier.com/locate/ijhff

Correlations for modeling transitional boundary layers under influences of freestream turbulence and pressure gradient

Keerati Suluksna [a], Pramote Dechaumphai [b], Ekachai Juntasaro [a,*,1]

[a] School of Mechanical Engineering, Institute of Engineering, Suranaree University of Technology, Nakhon Ratchasima 30000, Thailand
[b] Department of Mechanical Engineering, Faculty of Engineering, Chulalongkorn University, Bangkok 10330, Thailand

ARTICLE INFO

Article history:
Received 24 January 2007
Received in revised form 8 July 2008
Accepted 16 September 2008
Available online 13 November 2008

Keywords:
Transition model
Critical momentum thickness Reynolds number
Boundary layer
Freestream turbulence
Transition length parameter
Pressure gradient

ABSTRACT

This paper presents mathematical expressions for two significant parameters which control the onset location and length of transition in the γ–Re_θ transition model of Menter et al. [Menter, F.R., Langtry, R.B., Volker, S., Huang, P.G., 2005. Transition modelling for general purpose CFD codes. In: ERCOFTAC International Symposium on Engineering Turbulence Modelling and Measurements]. The expressions are formulated and calibrated by means of numerical experiments for predicting transitional boundary layers under the influences of freestream turbulence and pressure gradient. It was also found that the correlation for transition momentum thickness Reynolds number needs only to be expressed in terms of local turbulence intensity, so that the more complex form that includes pressure gradient effects is unnecessary. Transitional boundary layers on a flat plate both with and without pressure gradients are employed to assess the performance of these two expressions for predicting the transition. The results show that the proposed expressions can work well with the model of Menter et al. (2005).

1. Introduction

It has been reported in the literature that most boundary layer flows in turbomachines include a transitional flow regime unless they are tripped at the leading edge of the blade. In the past, the boundary layer prediction for turbomachinery blades frequently ignored the transition region and considered transition as a sudden-change event. In fact, the transition zone is quite large compared to the size of the body surface under consideration. In some cases, the proportion of the transitional boundary layer can be as high as 80% of the blade surface (Brown and Burton, 1978; Krishnamoorthy, 1986; Lardeau et al., 2005). Transition can, therefore, be viewed as a dominant part of the flow in turbomachines with a large effect on design parameters. In turbomachinery design, two important parameters are the coefficients of skin friction and heat transfer. Both coefficients increase significantly when the transition of the boundary layer from the laminar state to the turbulent one occurs. The increased skin friction results in increased losses. Turbomachines properly designed with the transition zone will operate with lower losses and a reduced chance of boundary layer separation. Furthermore, consideration of transition allows the accurate prediction of heat transfer coefficient, which is important for the design of turbine blades operating at high temperature. These design refinements permit the size of blades and the number of blades and stages to be reduced, with a resulting positive impact on the performance, weight and cost of turbomachine. Therefore, the prediction of transition is an important element in design and analysis of more efficient turbomachinery systems (Langtry and Menter, 2005).

Flow transition is a complex phenomenon that is difficult to predict accurately. A complete theory on transition does not exist to date. The ability of low-Reynolds-number turbulence models to predict the transition is questionable. Most of these models rely on damping functions to reproduce the viscous sublayer behavior, a capability that does not extend to the prediction of boundary layer transition (Menter et al., 2005). Many research groups in the last decade have concluded that two-equation turbulence models are deficient since they tend to predict a transition onset that is too early and a transition length that is too short.

An alternative approach is to blend the flow from the laminar state to the turbulent one using the concept of intermittency. Intermittency is a factor that is defined as the fraction of time that the flow is turbulent during the transition phase. It is normally defined as zero in the laminar region and unity in the fully turbulent region, and may be derived from experiments. A well-known correlation for the intermittency in the streamwise direction was proposed by Dhawan and Narasimha (1958). Another popular

* Corresponding author. Tel.: +66 89 8971657; fax: +66 44 224613/2 9132773.
E-mail addresses: junta@sut.ac.th, junta@g.sut.ac.th, e_juntasaro@hotmail.com (E. Juntasaro).
[1] Address: The Sirindhorn International Thai-German Graduate School of Engineering (TGGS), King Mongkut's University of Technology North Bangkok, 1518 Pracharaj Sai 1 Road (Pibulsongkram Road), Bangsue, Bangkok 10800, Thailand.

0142-727X/$ - see front matter © 2008 Elsevier Inc. All rights reserved.
doi:10.1016/j.ijheatfluidflow.2008.09.004

one for the cross-stream direction was proposed by Klebanoff (1955). During the last decade, intermittency has been modeled with a transport equation for use in general purpose CFD codes. For example, the transport equations for intermittency were proposed by Suzen and Huang (2000), Steelant and Dick (2001), Menter et al. (2002), Pecnik et al. (2003) and Lodefier and Dick (2005). To model transition, two important parameters are the onset location and length of transition. The onset of transition can be specified by a correlation, generally related to the transition momentum thickness Reynolds number, $Re_{\theta t}$. The length of transition is usually expressed implicitly in terms of the growth rate parameter and a model function. However, the main shortcoming of most transition models is that they are developed based on non-local variables. This is not appropriate for modern CFD methods in which unstructured grids and parallel computing are used.

In the present paper, the γ–Re_θ transition model of Menter et al. (2005) is investigated. This model is developed based on local variables which are compatible with modern CFD methods. The transport equation for the intermittency contains two specific parameters, F_{length} and F_{onset}. F_{length} is used to control the length of the transition region while F_{onset} is used to control the onset location of the transition. At present, these parameters are proprietary and their formulae are unpublished. The aim of this paper is to propose mathematical expressions for these specific parameters in order to close the model. It is believed that the proposed expressions are valid for both natural and bypass transition in boundary layers with and without pressure gradient.

2. γ–Re_θ transition model of Menter et al. (2005)

The γ–Re_θ transition model of Menter et al. (2005) consists of two transport equations: the equation for the intermittency, γ, and the equation for the transition momentum thickness Reynolds number, $Re_{\theta t}$, which is formulated in terms of the scalar quantity, $\widetilde{Re}_{\theta t}$. The γ-equation is used to trigger the transition process and the $\widetilde{Re}_{\theta t}$-equation is employed to avoid non-local variables. Both transport equations are written as

$$\frac{\partial \rho u_j \gamma}{\partial x_j} = P_{\gamma 1} + P_{\gamma 2} + \frac{\partial}{\partial x_j}\left[\left(\mu + \frac{\mu_t}{\sigma_\gamma}\right)\frac{\partial \gamma}{\partial x_j}\right], \tag{1}$$

$$\frac{\partial \rho u_j \widetilde{Re}_{\theta t}}{\partial x_j} = P_{\theta t} + \frac{\partial}{\partial x_j}\left[\sigma_{\theta t}(\mu + \mu_t)\frac{\partial \widetilde{Re}_{\theta t}}{\partial x_j}\right], \tag{2}$$

where ρ is the density, u_j is the velocity vector, μ is the molecular viscosity, and μ_t is the eddy viscosity.

The production terms, $P_{\gamma 1}$, $P_{\gamma 2}$ and $P_{\theta t}$ are defined as follows:

$$P_{\gamma 1} = (1 - c_{e1}\gamma)F_{\text{length}} c_{a1}\rho S(\gamma F_{\text{onset}})^{c_\alpha},$$
$$P_{\gamma 2} = (1 - c_{e2}\gamma)c_{a2}\rho\Omega\gamma F_{\text{turb}}, \tag{3a, b}$$

$$P_{\theta t} = c_{\theta t}\frac{(\rho U)^2}{500\mu}(Re_{\theta t} - \tilde{Re}_{\theta t})(1 - F_{\theta t}), \tag{4}$$

where S is the strain rate magnitude, Ω is the vorticity magnitude, and U is the local velocity magnitude. The parameters F_{length} and F_{onset} are used to control the length and onset location of transition, respectively. F_{turb} and $F_{\theta t}$ are the parameters for controlling the destruction/relaminarization of the boundary layer and the boundary layer detector, respectively.

The modeled transport equations are controlled by the following functions:

$$F_{\text{onset}} = \max[F_{\text{onset2}} - F_{\text{onset3}}; 0], \quad F_{\text{turb}} = \exp[-(R_T/4)^4], \tag{5a, b}$$

$$F_{\text{onset2}} = \min[\max[F_{\text{onset1}}; F_{\text{onset1}}^4]; 2], \quad F_{\text{onset1}} = \frac{Re_v}{2.193 Re_{\theta c}}, \tag{6a, b}$$

$$F_{\text{onset3}} = \max[1 - (R_T/2.5)^3; 0], \tag{7}$$

$$F_{\theta t} = \min\left[\max\left[F_{\text{wake}} \cdot \exp\left[-\left(\frac{y_n}{\delta}\right)^4\right]; 1 - \left(\frac{c_{e2}\gamma - 1}{c_{e2} - 1}\right)^2\right]; 1\right],$$
$$F_{\text{wake}} = \exp\left[-\left(\frac{Re_\omega}{10^5}\right)^2\right], \tag{8a, b}$$

$$Re_v = \frac{\rho S y_n^2}{\mu}, \quad R_T = \frac{\rho k}{\mu\omega}, \quad Re_\omega = \frac{\rho\omega y_n^2}{\mu},$$
$$\delta = \frac{50\Omega y_n}{U}\delta_{BL}, \quad \delta_{BL} = \frac{15\theta_{BL}}{2}, \quad \theta_{BL} = \frac{\tilde{Re}_{\theta t}\mu}{\rho U}, \tag{9a-f}$$

where y_n is the normal distance from the nearest wall, k is the turbulence kinetic energy, and ω is the specific dissipation rate of k. Re_v and R_T are the vorticity Reynolds number and the viscosity ratio, respectively. $Re_{\theta c}$ is the critical momentum thickness Reynolds number where the intermittency first appears in the boundary layer.

The model constants are $c_{a1} = 2$, $c_{e1} = 1$, $c_{a2} = 0.06$, $c_{e2} = 50$, $c_\alpha = 0.5$, $\sigma_\gamma = 1$, $\sigma_{\theta t} = 2$, and $c_{\theta t} = 0.03$. $Re_{\theta t}$ is calculated locally from the empirical correlation proposed by Menter et al. (2005). This parameter is related to the local turbulence intensity, Tu, and the pressure effect parameter, $F_{\lambda,K}$, as follows:

$$Re_{\theta t} = 803.73(\text{Tu} + 0.6067)^{-1.027} F_{\lambda,K}, \tag{10}$$

$$F_{\lambda,K} = \begin{cases} 1 + F_\lambda \cdot e^{-\text{Tu}/3}; & \lambda \leqslant 0 \\ 1 + F_K \cdot (1 - e^{-2Tu/3}) & \\ \quad +0.556(1 - e^{-23.9\lambda}) \cdot e^{-\text{Tu}/3}; & \lambda > 0 \end{cases}, \tag{11}$$

$$\lambda = \frac{\rho\theta^2}{\mu}\cdot\frac{dU}{ds}, \quad K = \frac{\mu}{\rho U^2}\cdot\frac{dU}{ds}, \quad \text{Tu} = \frac{100(2k/3)^{1/2}}{U}, \tag{12a-c}$$

where λ is the pressure gradient parameter, θ is the momentum thickness, K is the acceleration parameter, and dU/ds is the local acceleration in the streamline direction. The functions in the pressure effect parameter are defined as

$$F_\lambda = 10.32\lambda + 89.47\lambda^2 + 265.51\lambda^3, \tag{13a}$$
$$F_K = 0.0962(K \cdot 10^6) + 0.148(K \cdot 10^6)^2 + 0.0141(K \cdot 10^6)^3. \tag{13b}$$

To evaluate $Re_{\theta t}$ in Eq. (10), the calculation procedure must be performed iteratively because λ is not known in advance. The procedure starts from setting $\lambda = 0$ in order to calculate the $F_{\lambda,K}$ and $Re_{\theta t}$ and then calculating θ from its definition $\theta = (\mu/\rho U)\, Re_{\theta t}$. To avoid unstable computation during the iteration, the values of λ and $Re_{\theta t}$ should be bounded within the ranges of $-0.1 \leqslant \lambda \leqslant 0.1$ and $Re_{\theta t} \geqslant 20$.

This transition model has been calibrated for use in accordance with the SST turbulence model as follows:

$$\widetilde{P}_k = \gamma_{\text{eff}} P_k, \quad \widetilde{D}_k = \min[\max[\gamma_{\text{eff}}; 0.1]; 1] D_k, \tag{14a, b}$$

$$\tilde{f}_1 = \max[f_1; f_3], \tag{15}$$

where f_1 is the original blending function responsible for switching between the k–ω and k–ε models. P_k and D_k are the production and destruction terms of the turbulence kinetic energy equation in the original SST turbulence model respectively. The effective intermittency, γ_{eff}, is obtained from

$$\gamma_{\text{eff}} = \max[\gamma; \gamma_{\text{sep}}], \tag{16}$$

$$\gamma_{\text{sep}} = \min\left[2\max\left(\frac{Re_v}{3.235 Re_{\theta c}} - 1; 0\right) F_{\text{reattach}}; 2\right] F_{\theta t}, \tag{17}$$

$$F_{\text{reattach}} = \exp[-(R_T/20)^4], \quad f_3 = \exp[-(R_y/120)^8],$$
$$R_y = \rho y_n k^{1/2}/\mu. \tag{18a-c}$$

The boundary condition for the intermittency factor γ at freestream, outlet and wall is zero flux ($\partial\gamma/\partial n = 0$). At inlet, $\gamma = 1$ is applied. For $\widetilde{Re}_{\theta t}$, the boundary condition at freestream, outlet and wall is the zero flux ($\partial\widetilde{Re}_{\theta t}/\partial n = 0$). At inlet, the boundary condition for $\widetilde{Re}_{\theta t}$ can be specified by setting $\theta = 0$ (hence $\lambda = 0$ and $F_{\lambda,K} = 1$) and setting Tu with the value of freestream turbulence intensity at inlet and then substituting them into Eq. (10). The initial conditions for both γ and $\widetilde{Re}_{\theta t}$ are set to their inlet values. For turbulence model variables, the boundary conditions at inlet are $k = 1.5(\text{Tu}_{\text{in}} \cdot U_{\text{in}})^2$ and $\omega = \rho k/\mu_t$. At walls, $k = 0$ and $\omega = 60\mu/\rho\alpha_1 d_1^2$ are applied, where d_1 is the distance of the first node from the wall.

3. New correlations for the γ–Re_θ transition model

The main obstacle to employing the γ–Re_θ transition model of Menter et al. (2005) is the omission of two significant parameters in the transport equation of the intermittency: the transition length parameter, F_{length}, and the transition onset parameter, F_{onset} (see Eq. (3a)). The parameter F_{onset} has been formulated in terms of the vorticity Reynolds number, Re_v, and the critical momentum thickness Reynolds number, $Re_{\theta c}$ (not the transition momentum thickness Reynolds number, $Re_{\theta t}$, as usually found). Actually, $Re_{\theta c}$ for boundary layer flows can be analyzed from the linear-stability theory. Wilcox (1993) shows that the minimum critical Reynolds number of the Blasius boundary layer occurs at $Re_{xc} = 90{,}000$. This value corresponds to $Re_{\theta c} = 163$ as observed by Abu-Ghannam and Shaw (1980). However, based on $Re_{xc} = 90{,}000$, the experimental data reveal that the increase in the freestream turbulence level increases $Re_{\theta c}$ but decreases $Re_{\theta t}$ (see Table 1). In the case of high freestream turbulence levels, e.g., 7.78%, $Re_{\theta c}$ becomes larger than $Re_{\theta t}$. This seems not to be reasonable from the viewpoint of the flow physics because the critical location must necessarily be located upstream of the transition onset location. As a result, $Re_{\theta c}$ must not exceed $Re_{\theta t}$.

In the γ–Re_θ transition model of Menter et al. (2005), the parameter $Re_{\theta c}$ is imposed in the function of F_{onset}, Eq. (6b). This parameter refers to the location where the intermittency first starts to increase in the boundary layer. The increase in $Re_{\theta c}$ decreases the parameter F_{onset}. This influence induces a delay in the onset of transition. The decrease in $Re_{\theta c}$ increases the parameter F_{onset}, and hence the early onset of transition is obtained. The effect of the parameter F_{length} is incorporated into the intermittency transport equation via the production term, Eq. (3a). It can be seen that an increase in F_{length} increases the production term, resulting in a larger value of the intermittency. This gives rise to an increase in the effect of turbulence. This influence induces the rapid growth rate of the transition leading to a shorter transition length. On the other hand, a decrease in F_{length} decreases the turbulence effect, slowing the growth rate of the transition and leading to a longer transition length. Therefore, F_{length} controls the transition length by an inverse process. In other words, the larger F_{length}, the shorter the transition length, but the smaller F_{length}, the longer the transition length.

No information has been given in any previous publications for either $Re_{\theta c}$ or F_{length}. To close the model, mathematical expressions for these parameters must be specified. In the present work, the expressions for both $Re_{\theta c}$ and F_{length} are given as functions of $Re_{\theta c} = f(\widetilde{Re}_{\theta t})$ and $F_{\text{length}} = f(\widetilde{Re}_{\theta t})$. From the experimental data, it can be observed that the magnitudes of $Re_{\theta c}$ and $Re_{\theta t}$ are found to be in the same order (see Table 1). That is, the function for expressing the variation of $Re_{\theta c}$ with respect to $Re_{\theta t}$ should be in the form of a low-order polynomial, preferably linear for simplicity. The explicit form of the F_{length} function is much less intuitive. In the calibration procedure developed herein, the starting point is setting $Re_{\theta c} = a_{\theta t}\widetilde{Re}_{\theta t}$, and $F_{\text{length}} = b_{\text{length}}$, where $a_{\theta t}$ and b_{length} are constants. Typical starting values would be $a_{\theta t} = 0.8$ and $b_{\text{length}} = 100$. The value of b_{length} is varied to correspond the profile shape of the skin friction coefficient with the experimental data. When the corresponding shape is obtained, the next step is to match the location of the shape with the experimental data. At this step, the shape must be moved to the correct location. F_{length} obtained from the previous step is now fixed. Then the value of $Re_{\theta c}$ that controls the shape location is adjusted via the constant $a_{\theta t}$ until the correct location is found. The procedure for this numerical experiment for determining $Re_{\theta c}$ and F_{length} is shown in Fig. 1. It can be seen that the larger F_{length}, the shorter the transition length manifested by the rapid growth of the skin friction coefficient. A small value of $Re_{\theta c}$ results in an earlier transition onset while a larger value results in a delayed transition. In the example of Fig. 1,

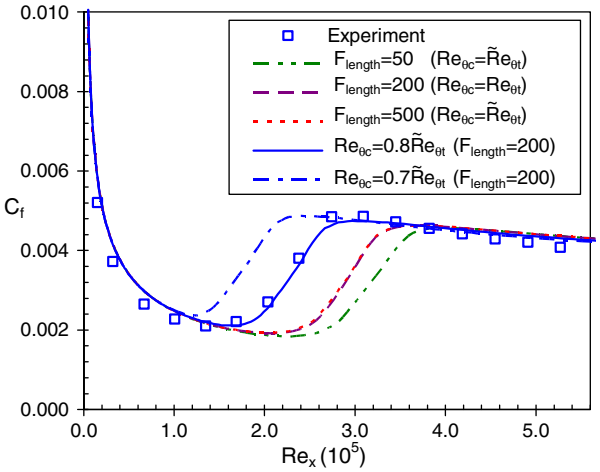

Fig. 1. Numerical experiments to match the skin friction coefficient profile shape with the experimental data.

Table 1
Summary of the experimental/numerical data of all T3 test cases

Case	U_{in} (m/s)	Tu_{in} (%)	R_T	Re_L Exp	$Re_{\theta t}/Re_{\theta c}$ Exp	x_S/x_E (mm)			
						Exp	LS	SH	Menter
T3C1	5.9	7.78	44.0	7.72×10^5	211/250	195/495	125/207	65/172	183/400
T3C2	5.0	3.10	9.0	6.58×10^5	377/209	795/1295	370/640	640/981	940/1194
T3C3	3.7	3.10	6.0	4.77×10^5	519/217	1195/–	617/1010	1010/1280	1195/- -
T3C4	1.2	3.10	2.5	1.36×10^5	381/165	1395/-	1420/–	1417/-	1345/–
T3C5	8.4	3.70	15.0	1.09×10^6	332/164	345/645	196/331	353/545	353/688

Note: The $Re_{\theta c}$ above is determined from the experimental data based on the critical Reynolds number of 90,000. Exp; experimental data, LS; Launder and Sharma (1974), SH; Suzen and Huang (2000) and Menter; Menter et al. (2005).

the best-matched shape is found at $Re_{\theta c} = 0.8\widetilde{Re}_{\theta t}$ and $F_{\text{length}} = 200$.

The procedure described above to calibrate the $Re_{\theta c}$ and F_{length} functions has been applied to the ERCOFTAC zero pressure gradient cases T3AM, T3A and T3B for bypass transition. To extend this calibration to natural transition, the zero pressure gradient data of Schubauer and Klebanoff (1955) (TSK case) with $Tu_{in} = 0.18\%$ and $\mu_t/\mu = 5$ as shown in Fig. 2 was used. After the information for four cases above were obtained, the functions for the expressions $Re_{\theta c}$ and F_{length} were formulated using the method of data fitting. These functions may be fine tuned until the numerical results for all test cases agree well with the experimental data. The final relations of F_{length} and $Re_{\theta c}$ with $\widetilde{Re}_{\theta t}$ are shown in Fig. 3, and their formulations are expressed as follows:

$$Re_{\theta c} = \min[\max[-(0.025\widetilde{Re}_{\theta t})^2 + 1.47\widetilde{Re}_{\theta t} - 120; 125]; \widetilde{Re}_{\theta t}], \quad (19)$$

$$F_{\text{length}} = \min[0.1\exp(-0.022\widetilde{Re}_{\theta t} + 12) + 0.45; 300], \quad (20)$$

where $\widetilde{Re}_{\theta t}$ is the local transition momentum thickness Reynolds number evaluated from Eq. (2).

From Fig. 3, the expression for $Re_{\theta c}$ corresponding to the Menter et al. (2005) model is constructed as a quadratic function of $\widetilde{Re}_{\theta t}$, Eq. (19). This function has been adjusted close to the profile of $Re_{\theta c} = \widetilde{Re}_{\theta t}$ for high freestream turbulence Tu > 5.5%, corresponding to $\widetilde{Re}_{\theta t} < 125$. This is because, for high freestream turbulence level, the flow is dominated by the effect of bypass transition leading to the critical location close to the transition onset location. Furthermore, to retain the realistic nature of flow transition, $Re_{\theta c}$ must be restricted to not exceed $\widetilde{Re}_{\theta t}$. As a result, the profile of $Re_{\theta c} = \widetilde{Re}_{\theta t}$ can be viewed as the upper bound of $Re_{\theta c}$, and the minimum value of $Re_{\theta c}$ is limited by the minimum allowable value of $\widetilde{Re}_{\theta t} = 20$.

The transition length parameter, F_{length}, is displayed against $\widetilde{Re}_{\theta t}$ on a semi-logarithmic scale. The valid relation of F_{length} with $Re_{\theta t}$ is found to be an open zone for the boundary layer flow with Tu > 1% ($\widetilde{Re}_{\theta t} < 500$), and then become a single line for the boundary layer flow with Tu < 1% ($\widetilde{Re}_{\theta t} > 500$) (Suluksna and Juntasaro, 2008). The expression for F_{length} decreases exponentially with $\widetilde{Re}_{\theta t}$. Its function is chosen as a single line bordering the lower bound of the banded zone. The reasons are that it is convenient and gives rapid convergence in computations. Furthermore, the lower bound of F_{length} is set to 0.45 in order to ensure sufficient production for natural transition. It should be noted that the correlations for F_{length} and $Re_{\theta c}$ proposed in this paper are only the successful ones compatible with the model of Menter et al. (2005). These parameters are strongly sensitive to the boundary conditions and the boundary layer edge definition, which depends on the searching technique. In the present work the boundary layer edge is defined at $y = 2\delta\,(x)$.

In the present work, it is hypothesized that the pressure effect parameter, $F_{\lambda,K}$, in the correlation of $Re_{\theta t}$, Eq. (10), should be omitted, since the effects of pressure gradient are largely canceled by the decay of the local turbulence intensity, Tu. As illustrated in Fig. 4, this hypothesis is explained further as follows. A favorable pressure gradient (FPG) reduces the turbulence of the flow, leading to decrease in the turbulence intensity. The decrease in turbulence intensity increases the transition momentum thickness Reynolds number in Eq. (10), and hence moves the transition onset downstream. On the other hand, for an adverse pressure gradient (APG), the flow is decelerated, resulting in an increased turbulence intensity. The increase in turbulence intensity decreases the momentum thickness Reynolds number and the onset of transition moves upstream.

The correlations for transition momentum thickness Reynolds number, $Re_{\theta t}$, illustrated in Fig. 5 are based on zero pressure gradient (ZPG) condition and freestream turbulence intensity at the leading edge, Tu_{lde}, not the local freestream turbulence intensity. To apply to non-zero pressure gradient (NZPG) cases, in general, these correlations would be multiplied by the pressure effect parameter, that is $Re_{\theta t,\text{NZPG}} = Re_{\theta t,\text{ZPG}} \cdot F_{\lambda,K}$. In the present work, the

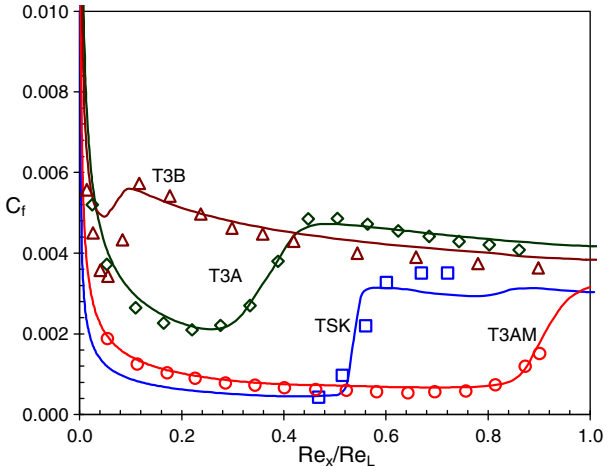

Fig. 2. Skin friction coefficient for Schubauer and Klebanoff (1955) and ZPG cases.

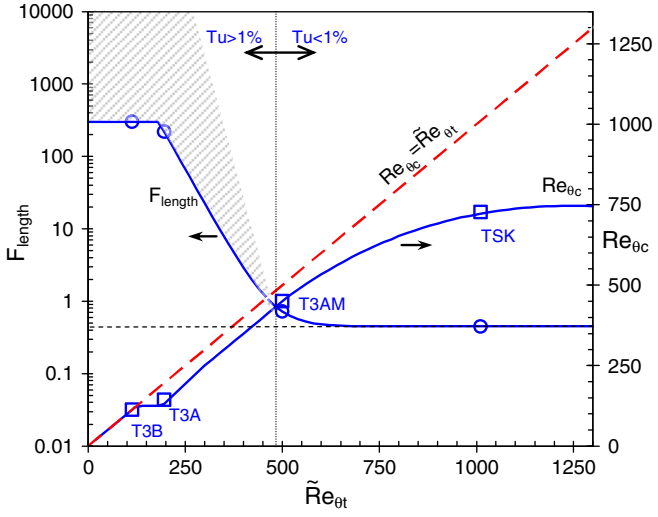

Fig. 3. Relations of $Re_{\theta c}$ and F_{length} with $\widetilde{Re}_{\theta t}$.

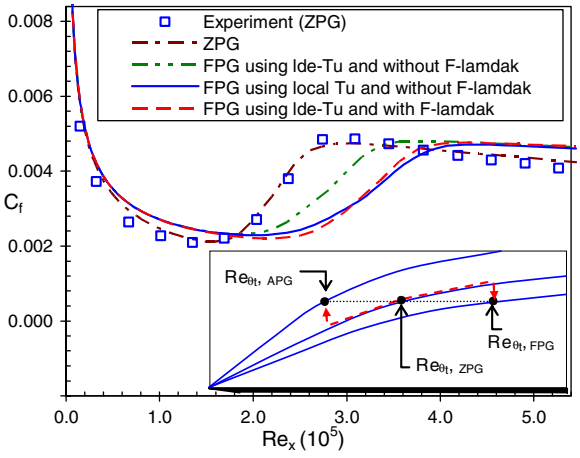

Fig. 4. Hypothesis for the omission of pressure gradient effect.

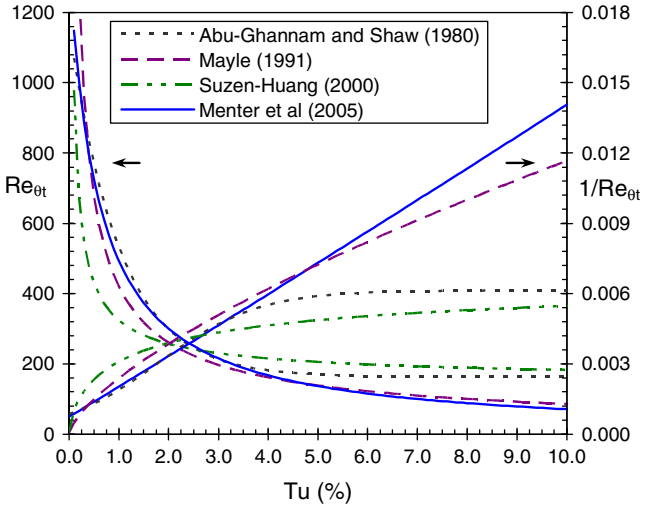

Fig. 5. Relations of $Re_{\theta t}$ with Tu under ZPG condition. (See above-mentioned references for further information.)

local turbulence intensity, Tu, is used rather than the leading edge value, Tu_{lde}, for calculating $Re_{\theta t}$. As illustrated in Fig. 4, the use of the local turbulence intensity is a proxy for the use of $F_{\lambda,K}$ in combination with the leading edge value. In this way, the effect of pressure gradient is implicitly absorbed in the local turbulence intensity. Therefore, the pressure effect parameter, $F_{\lambda,K}$, is not needed to calculate the transition momentum thickness Reynolds number using local turbulence intensity.

4. Computation procedure

Test cases presented in this paper are the ERCOFTAC T3-series of flat plate experiment that are commonly used as a benchmark for the transition prediction by turbulence models. As mentioned earlier, the zero pressure gradient cases T3AM, T3A and T3B are used for the model calibration for bypass transition, together with the TSK (Schubauer and Klebanoff, 1955) case allow freestream turbulence level of 0.18% for natural transition. In addition, the T3C series cases combine the influences of freestream turbulence and favorable/adverse pressure gradient imposed by the opposite converging/diverging wall, The T3C1, T3C2, T3C3 and T3C5 cases are specifically designed for testing the ability of turbulence models to predict transition under the continuous variation of pressure gradient representing an aft-loaded turbine blade (Suzen and Huang, 2001). The T3C4 case is usually used to test the model ability to predict the separation-induced transition (Langtry and Menter, 2005).

The domain consists of a flat plate bottom wall of 1.7 m. long and a variable-height upper wall. At the entrance, the gap between the upper and bottom walls is 0.3 m. and this gap varies along the streamwise direction corresponding to the experimental data of the pressure gradient variation. The computational domain begins at 0.15 m. upstream of the plate leading edge to eliminate an ambiguous specification of freestream conditions. In the present work, a grid-independence check was performed, in which the grid spacing was decreased by half in both directions. The first node adjacent to the wall is controlled to locate at $0.001 < y^+ < 0.01$. A mesh of 135 (streamwise) $\times$ 125 (expanding from wall to freestream) is found to be the best, and is adopted for all test cases.

In the computation, incompressible flow is considered. The fluid density and the molecular viscosity are specified with the constant values of 1.2 kg/m^3 and 1.8×10^{-5} kg/m s, respectively. The Reynolds number, Re_x, is based on the plate length and local freestream velocity. The SIMPLE algorithm is employed to solve all transport equations. Computations are performed by an elliptic solver to solve the mean flow, turbulence and transition model equations. A second-order upwind scheme and the finite volume discretization are employed. The inlet conditions are prescribed to reproduce the experimental decay of the freestream turbulence intensity. Isotropic turbulence is assumed so that the inlet turbulence kinetic energy can be obtained from the experimental inlet freestream turbulence level. The inlet viscosity ratio, R_T, is specified in order to mimic the experimentally measured decay of the freestream turbulence intensity as shown in Fig. 6. Hence, the inlet conditions for the turbulent variables are calculated from the following relations:

$$\mu_t = R_T \mu, \quad k = (3/2)(\mathrm{Tu}_{\mathrm{in}} \cdot U_{\mathrm{in}})^2, \quad \omega = \rho k/\mu_t, \tag{21}$$

where $\mathrm{Tu}_{\mathrm{in}}$ denotes the inlet freestream turbulence level (%), and U_{in} is the inlet velocity. At the outlet boundary, all variables are extrapolated from nodes inside the domain to the boundary. Details of inlet conditions of all test cases are given in Table 1.

Generally, it is not difficult to obtain the appropriate value for the inlet viscosity ratio that reproduces the experimental decay of the freestream turbulence intensity. Such a value can be found by least square curve fits based on the analytical decay laws derived from the SST k–ω turbulence model, or by numerical experiments. To find out the domain shape that can reproduce the required pressure gradient the local freestream velocity, known from the experimental data, was used to compute the width of each cross-section along the flow direction from continuity. The profiles of the domain width and the grid configuration are shown in Fig. 7, where h is the domain width, D is the inlet domain width, U_{fst} is the local freestream velocity and U_{in} is the inlet velocity. It can be seen that the domain cross-section initially converges and then subsequently diverges. In other words, the pressure gradient is negative (favorable) for $x < 0.9$ m, and becomes positive (adverse). The domain width profile for the T3C4 case is given by Eq. (22) while the profile for the rest of T3C cases is expressed by Eq. (23):

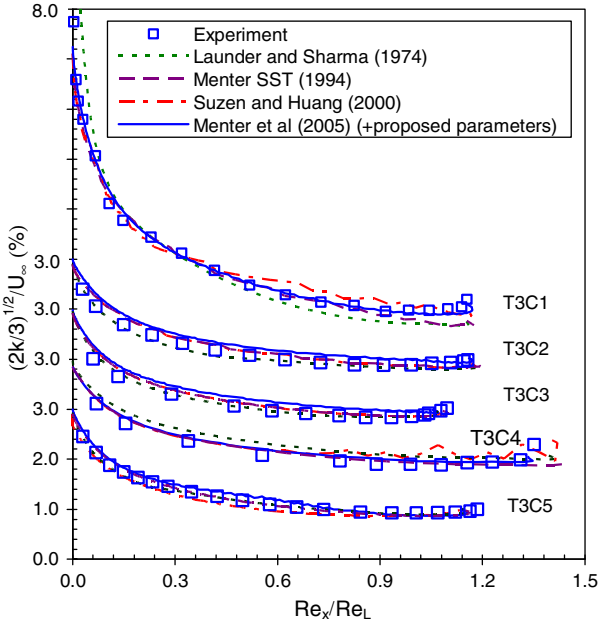

Fig. 6. Freestream turbulence intensity decay for T3C cases.

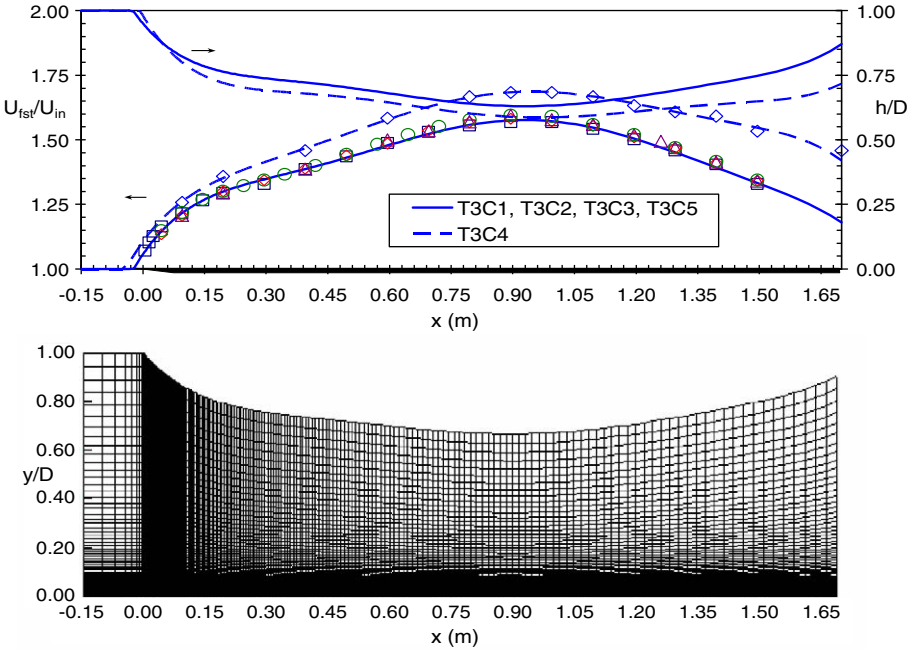

Fig. 7. Normalized domain thickness and normalized freestream velocity (top) and grid configuration (bottom) for T3C cases.

$$h/D = \min[1.356x^6 - 7.591x^5 + 16.513x^4 - 17.510x^3 + 9.486x^2 - 2.657x + 0.991; 1], \quad (22)$$

$$h/D = \min[1.231x^6 - 6.705x^5 + 14.061x^4 - 14.113x^3 + 7.109x^2 - 1.900x + 0.950; 1], \quad (23)$$

where x is the plate distance from the leading edge.

Due to the change of the cross-sectional area along the flow direction, the physical domain in case of non-zero pressure gradient is not rectangular in shape. To generate a mesh for such a non-rectangular shape, the transformation technique is adopted here to transform the physical space (x, y) to the computational space (ξ, η). The transformation is accomplished by specifying a generalized coordinate system that maps the curvilinear grid system in the physical space to a rectangular uniform grid system in the computational space. In the present work, the transformation technique used is the so-called inverse transformation. With this technique, the transformed governing equation is expressed in terms of the inverse metrics and the Jacobian.

5. Results and discussion

The predicted results by the transition model of Menter et al. (2005) with the proposed F_{length} and $Re_{\theta c}$ parameters are compared with the experimental data for the skin friction coefficient, C_f. This coefficient is an important indication of the starting and ending points of transition, and also the growth rate and length of transition. The variation of the skin friction coefficient along the flat plate is usually displayed with respect to the Reynolds number (linear-scale plots are displayed in this work). The start and end of transition occur at the points where the skin friction coefficient profile reaches the minimum and maximum values, respectively. The variation between these two points indicates the growth rate and length of transition (the more the rapid growth rate; the shorter the transition length). The start, x_S, and end, x_E, locations of the transition predicted by the models for all test cases are summarized in Table 1. Comparisons of the skin friction coefficient are illustrated in Fig. 2 for zero pressure gradient cases and in Figs. 8–12 for non-zero pressure gradient cases. Furthermore, the mean

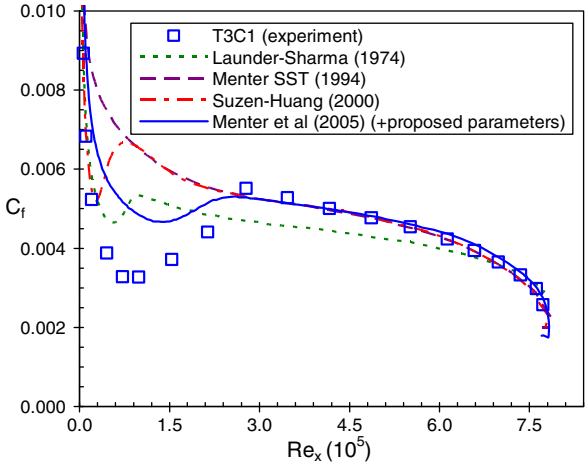

Fig. 8. Skin friction coefficient for T3C1 case.

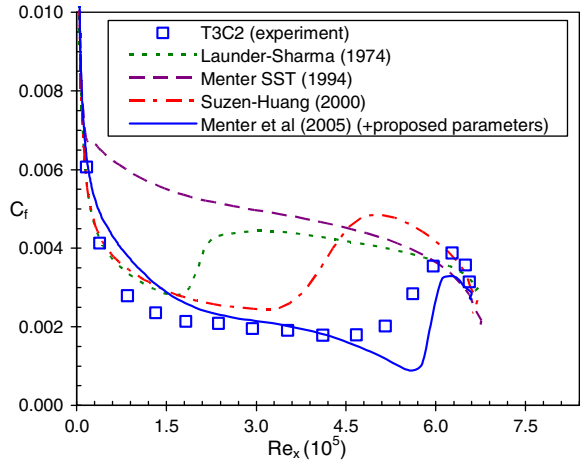

Fig. 9. Skin friction coefficient for T3C2 case.

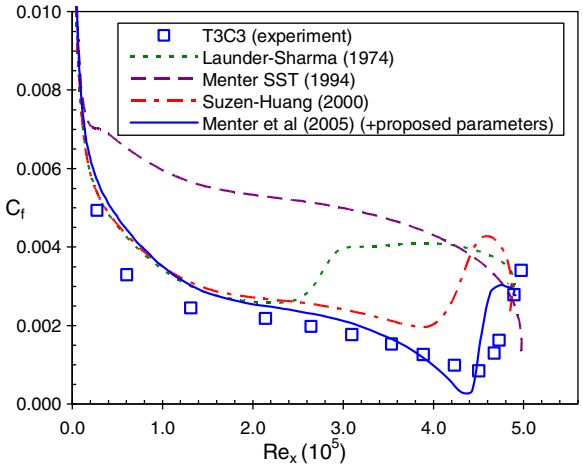

Fig. 10. Skin friction coefficient for T3C3 case.

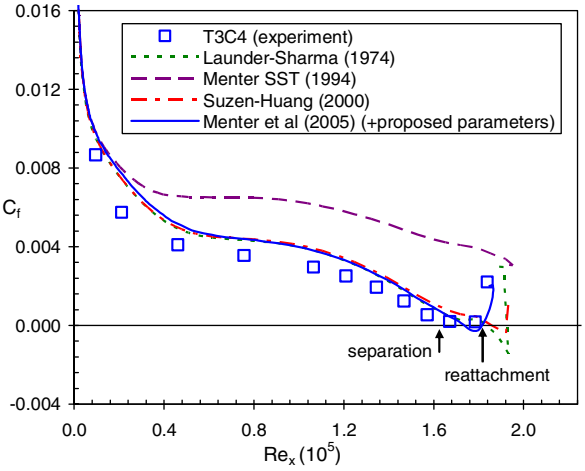

Fig. 11. Skin friction coefficient for T3C4 case.

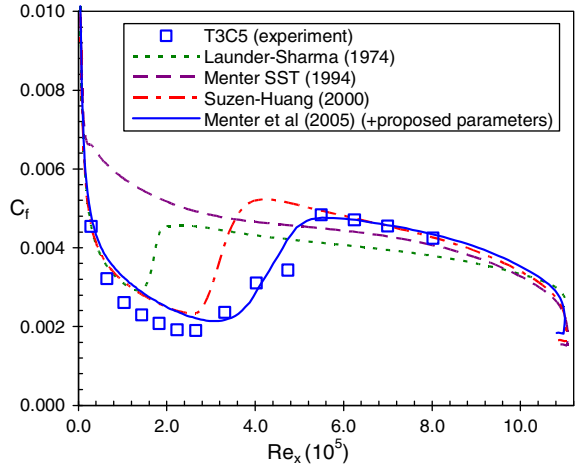

Fig. 12. Skin friction coefficient for T3C5 case.

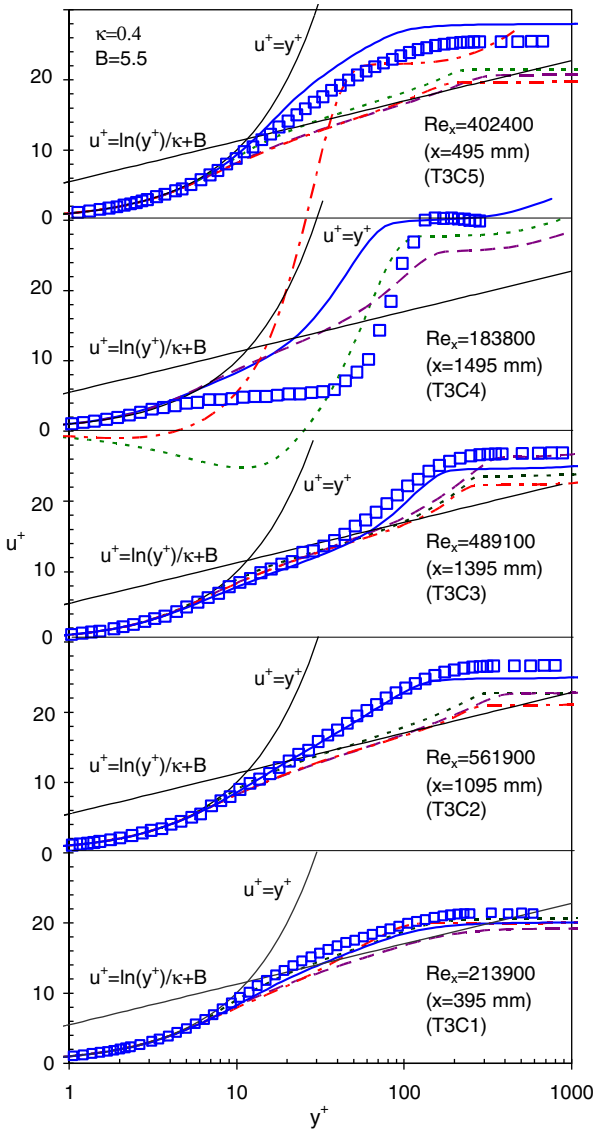

Fig. 13. u^+ vs. y^+ in the transition region for T3C cases. *Note:* experimental data; □. Predicted results: - - - -; Launder and Sharma (1974), — — ; Menter SST (1994), —— ; Suzen and Huang (2000), and — - — ; Menter et al. (2005) (+ proposed parameters).

velocity profile scaled in wall units, u^+, the Reynolds shear stress, $-\overline{u'v'} = v_t \partial u/\partial y$, and the turbulence kinetic energy, k, in the transition region are also presented in Figs. 13–15, respectively. The T3C test cases can be classified into two groups depending on the level of the freestream turbulence: moderate freestream turbulence levels, 1% < Tu < 3%, and high freestream turbulence levels, Tu > 3%. T3C1 is a high freestream turbulence level case, and the rest of T3C test cases are moderate freestream turbulence level cases.

The T3C1 case (Tu_{in} = 7.78%): high freestream turbulence intensity flow case. The predicted skin friction coefficient is compared with the experimental data in Fig. 8. The turbulence model of Menter (1994) without the benefit of a transition model predicts fully turbulent flow for the entire flow region without any transition behavior. The turbulence model of Launder and Sharma (1974) and the model of Suzen and Huang (2000) predict early onsets of transition and rapid variation of the skin friction coefficients in the transition region. The model of Menter et al. (2005) satisfactorily predicts the onset of transition but over-predicts the skin friction coefficient. This is because a large value of inlet viscosity ratio, R_T, has been specified to obtain the required freestream decay. For the mean velocity profiles, Fig. 13, all considered models give results that are comparable to the experimental data. The Reynolds shear stress in Fig. 14 shows slightly over-predicted results obtained from the turbulence model of Menter (1994) and the model

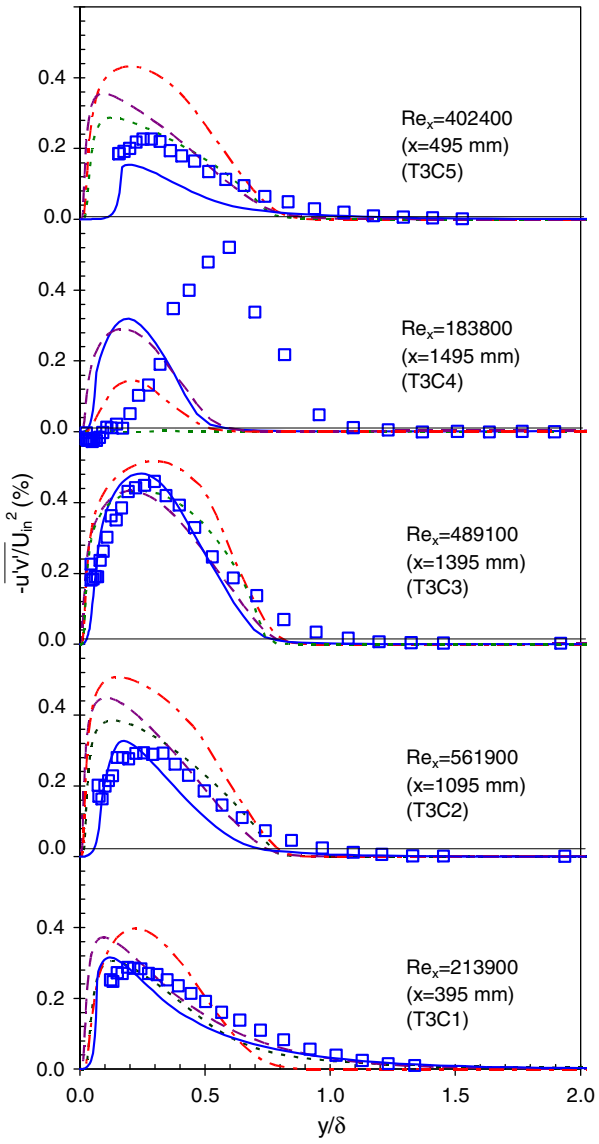

Fig. 14. $-\overline{u'v'}/U_{in}^2$ vs. y/δ in the transition region for T3C cases. *Note:* experimental data; □. Predicted results: - - - -; Launder and Sharma (1974), - - - - ; Menter SST (1994), — — ; Suzen and Huang (2000), and — - — ; Menter et al. (2005) (+ proposed parameters).

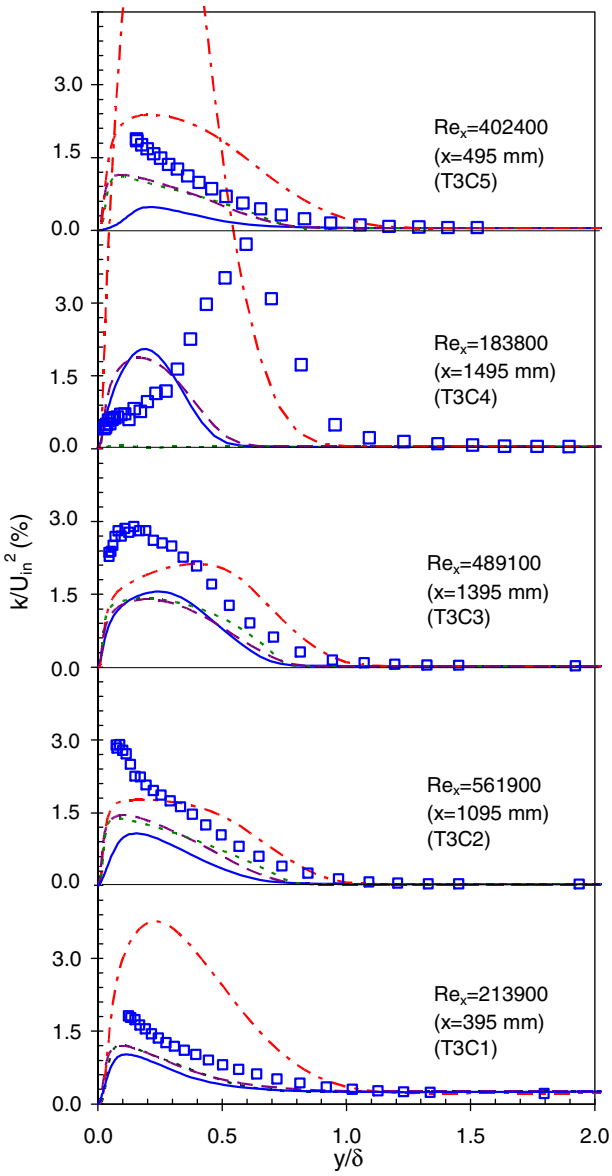

Fig. 15. k/U_{in}^2 vs. y/δ in the transition region for T3C cases. *Note:* experimental data; □. Predicted results: - - - -; Launder and Sharma (1974), - - - - ; Menter SST (1994), — — ; Suzen and Huang (2000), and — - — ; Menter et al. (2005) (+ proposed parameters).

of Suzen and Huang (2000), and fairly good results are obtained from the Menter et al. (2005) and Launder and Sharma (1974) models. As shown in Fig. 15, the model of Suzen and Huang (2000) over-predicts the turbulent kinetic energy while the other models tend to under-predict it.

The T3C2 case (Tu_{in} = 3.1%): moderate freestream turbulence intensity flow case. The predicted skin friction coefficient for this case is compared to the experimental data in Fig. 9. The turbulence model of Menter (1994) again predicts fully turbulent flow without displaying any transition behavior. The turbulence model of Launder and Sharma (1974) and the model of Suzen and Huang (2000) both predict early transition. The model of Menter et al. (2005), correctly predicts the location of the transition onset, but a shorter transition length is obtained than the experimental data. The mean velocity profile for this case is depicted in Fig. 13. It is found that only the Menter et al. (2005) model produces acceptable results, while the rest of the considered models tend to under-predict mean velocity. As shown in Fig. 14, the model of Menter et al. (2005) gives a fairly good result for the Reynolds shear stress, while the rest of the models considered tend to over-predict this quantity. All models considered under-predict the turbulence kinetic energy, as is illustrated in Fig. 15.

The T3C3 case (Tu_{in} = 3.1%): moderate freestream turbulence intensity flow case. The predicted skin friction coefficient is compared to the experimental data in Fig. 10. As can be seen from the figure, the result obtained from the turbulence model of Menter (1994) is fully turbulent and no effect of transition is captured. The turbulence model of Launder and Sharma (1974) and the model of Suzen and Huang (2000) again predict the location of transition onset that is too early. The model of Menter et al. (2005) gives a good prediction of skin friction coefficient compared with the experimental data. The predicted result shows the flow tendency towards incipient separation at location of transition onset. The mean velocity profile for this test case is illustrated in Fig. 13. Results obtained from the turbulence models of Menter (1994) and Launder and Sharma (1974), and the model of Suzen and Huang (2000) under-predicted the mean velocity for $y^+ > 50$ due to the

early transition prediction. The model of Menter et al. (2005), yields a very good result compared to the experimental data. The model of Suzen and Huang (2000) slightly over-predicts, the Reynolds shear stress, Fig. 14, while the results of the rest models considered agree well with the experimental data. All the models considered under-predict the turbulence kinetic energy when compared with the experimental data (see Fig. 15).

The T3C4 case (Tu_{in} = 3.1%): flow with separation-induced transition. In this case, the experimental data show that the boundary layer separates in the rear region of the flat plate at x = 1295 mm. and then reattaches at x = 1395 mm. A laminar separation bubble is formed and transition is induced by this separation. The predicted skin friction coefficient for this case is displayed in Fig. 11. It is found that the turbulence model of Menter (1994) predicts fully turbulent flow without separation. The turbulence model of Launder and Sharma (1974) and the model of Suzen and Huang (2000) predict the separation behavior of the boundary layer, but with a delayed separation location. The model of Menter et al. (2005) with the proposed parameters can simulate the separation behavior of the boundary layer with satisfactory locations of separation and reattachment, and also gives a good prediction of transition induced by the separation. For the mean velocity profile in the transition region, illustrated in Fig. 13, the model of Menter et al. (2005) gives a reasonable result compared with the experiment while the rest of considered models give unsatisfactory results. Comparisons of the Reynolds shear stress and turbulence kinetic energy are shown in Figs. 14 and 15. The results show that all considered models produce the maximum peak too early and the results are largely unsatisfactory.

The T3C5 case (Tu_{in} = 3.7%): transitional boundary layer flow with high Reynolds number. In this case, the experiment shows that transition occurs in the region of favorable pressure gradient. The predicted results for skin friction coefficient are shown in Fig. 12. Again, the turbulence model of Menter (1994) results in fully turbulent flow. The turbulence model of Launder and Sharma (1974) predicts an onset of transition that is too early and and the growth rate of transition that is too rapid. The model of Suzen and Huang (2000) predicts the satisfactory onset of transition but produces a growth rate of transition that is too rapid. With the model of Menter et al. (2005), the predicted result is in satisfactory agreement with the experiment. For the mean velocity profile, Fig. 13, the model of Menter et al. (2005) gives slightly over-predicted values while the rest of the models under-predict the profiles compared with the experimental data. The comparison of Reynolds shear stress is shown in Fig. 14. It is found that the model of Menter et al. (2005) under-predicts the profile, while the rest considered models over-predict it. The predicted turbulence kinetic energy is compared in Fig. 15. Only the model of Suzen and Huang (2000) over-predicts the turbulence kinetic energy, while all the other models under-predict them.

From the summary above, it can be concluded that the turbulence model of Menter (1994) always produces fully turbulent boundary layers and cannot detect any effect of transition in all test cases. The reason is that this model has been developed from a high-Reynolds-number turbulence model without any damping function to reproduce the viscous sublayer behavior. As a result, the model always gives the immediate variation of the skin friction coefficient to the turbulent profile at the leading edge of the flat plate. In case of separated flow, the model cannot detect the separation region and therefore the transition region induced by the separation does not appear.

The low-Reynolds-number k–ε turbulence model with the damping function of Launder and Sharma (1974) is capable of capturing the transition behavior. The laminar solution from the leading edge to the transition onset is obtained and the transition to turbulence is produced downstream. The model always gives an early onset location with too rapid growth rate of transition to turbulence leading to the shorter transition length when compared with the experimental data. This is because the damping function of this model has been developed to handle the near-wall region of turbulent flow, but is not calibrated for the prediction of transition. The capability to predict transition is just a by-product from their viscous sublayer formulation. The model can predict the separation behavior of the boundary layer with the delayed separation point and hence gives the fairly good result for the transition induced by the separation. However, for the skin friction coefficient, the model always predicts an undershoot result compare with the experimental data.

The model of Suzen and Huang (2000) predicts an early onset of transition and a rapid variation of the skin friction coefficient with the slight overshoot at the end of the transition region, which implies that the transition length is too short. For separated flow, the model can predict the separation of the flow and gives fairly good results for the transition effect induced by the separation.

The model of Menter et al. (2005) with proposed parameters gives satisfactory transition onset and length predictions for the case of moderate freestream turbulence levels. For the high freestream turbulence level case, the model gives the early start of the transition onset and cannot completely produce the behavior of the laminar boundary layer in the pre-transition region. As a result, this model is more proper for low and moderate freestream turbulence prediction than for high freestream turbulence prediction. For the case of separated flow, the model can simulate the separation behavior of the boundary layer with the satisfactory points of separation and reattachment, and also gives satisfactory results for the transition induced by the separation.

One advantage of the SST model of Menter (1994) and the k–ε model of Launder and Sharma (1974) is the rapid convergence rate compared with other considered models, since these models contain no transport equation for modeling the transition. In other words, only the transport equations for turbulence quantities are solved without any special modification. This saves computational time during the iteration. The main shortcoming of the Suzen and Huang (2000) model is the slow convergence rate compared with other relevant models. For the Menter et al. (2005) model, there are totally seven transport equations in this model to be solved for the two-dimensional transitional flow (two equations for mean flow, one equation for continuity (in form of p' equation), two equations for turbulence and two equations for transition). As a result, the computational time per iteration of this model is about 30% more than that of the SST model but about the same as that of the Suzen and Huang (2000) model.

6. Conclusion

The present paper proposes new expressions for two specific parameters, $Re_{\theta c}$ and F_{length}. $Re_{\theta c}$ is used to control the onset of transition and F_{length} is used to control the length of transition in the transition model of Menter et al. (2005). Those parameters are formulated by means of numerical experiments. The effect of pressure gradient on the transition of boundary layer is implicitly absorbed in the local turbulence intensity. Based on this concept, the correlation for specifying the onset of transition, i.e., the transition momentum thickness Reynolds number, $Re_{\theta t}$, is employed without the pressure effect parameter. The model with the proposed parameters is validated with the flat plate transitional boundary layer under the influences of freestream turbulence and pressure gradient of T3 series test cases. The results show that the Menter et al. (2005) model with the proposed parameters gives good agreement with the experiment for moderate freestream turbulence levels. For high freestream turbulence levels, the model gives

reasonably satisfactory results. For the separated-transition flow, the model with the proposed parameters can capture the separation of the flow and can predict a fairly realistic behavior of the transition induced by the separation.

Acknowledgements

This research is supported by the Thailand Research Fund (TRF) for the Senior Scholar Professor Dr. Pramote Dechaumphai. The authors would like to personally thank Dr. Y.B. Suzen, Dr. F.R. Menter, Dr. Koen Lodefier, Dr. Rene Pecnik and Dr. Paul Malan for their helpful discussion and papers during the course of this work.

References

Abu-Ghannam, B.J., Shaw, R., 1980. Natural transition of boundary layer: the effects of turbulence, pressure gradient, and flow history. J. Mech. Eng. Sci. 22, 213–228.

Brown, A., Burton, R.C., 1978. The effect of free stream turbulence intensity and velocity distribution on heat transfer to curved surfaces. ASME J. Eng. Power 100, 159–168.

Dhawan, S., Narasimha, R., 1958. Some properties of boundary layer during the transition from laminar to turbulent flow motion. J. Fluid Mech. 3, 418–436.

Klebanoff, P.S., 1955. Characteristics of turbulence in a boundary layer with zero pressure gradient. NACA Report No. 1247.

Krishnamoorthy, V., 1986. Effect of freestream turbulence on the convective heat transfer to gas turbine blades. Ph.D. thesis, Indian Institute of Technology, Bombay.

Langtry, R.B., Menter, F.R., 2005. Transition modeling for general CFD applications in aeronautics. AIAA, 2005–2522.

Lardeau, S., Li, N., Leschziner, M.A., 2005. LES of transitional boundary layer at high free-stream turbulence intensity and implications for RANS modelling, 431–436.

Launder, B.E., Sharma, B., 1974. Application of the energy dissipation model of turbulence to the calculation of flow near a spinning disk. Lett. Heat Mass Transfer 1, 131–138.

Lodefier, K., Dick, E., 2005. An unsteady RANS transition model with dynamics description of intermittency. In: Proceeding of ASME Turbo Expo 2005, Power for Land, Sea, and Air. Reno-Tahoe, Nevada, USA, June 16–19.

Mayle, R.E., 1991. The role of laminar-turbulent transition in gas turbine engines. ASME J. Turbomach. 113, 509–537.

Menter, F.R., 1994. Two-equation eddy-viscosity turbulence models for engineering applications. AIAA 32, 1598–1605.

Menter, F.R., Esch, T., Kubacki, S., 2002. Transition modelling based on local variables. In: Rodi, W., Fueyo, N. (Eds.), Engineering Turbulence Modelling and Experiments-5, pp. 555–564.

Menter, F.R., Langtry, R.B., Volker, S., Huang, P.G., 2005. Transition modelling for general purpose CFD codes. In: ERCOFTAC International Symposium on Engineering Turbulence Modelling and Measurements.

Pecnik, R., Sanz, W., Gehrer, A., Woisetschläger, J., 2003. Transition modeling using two different intermittency transport equation. Flow Turbul. Combust. 70, 299–323.

Schubauer, G.B., Klebanoff, P.S., 1955. Contribution on the mechanics of boundary layer transition. NACA TN 3489.

Steelant, J., Dick, E., 2001. Modeling of laminar-turbulent transition for high freestream turbulence. J. Fluids Eng. 123, 22–30.

Suluksna, K., Juntasaro, E., 2008. Assessment of intermittency transport equations for modeling transition in boundary layers subjected to freestream turbulence. Int. J. Heat Fluid Flow 29, 48–61.

Suzen, Y.B., Huang, P.G., 2000. Modeling of flow transition using an intermittency transport equation. J. Fluids Eng. 122, 273–284.

Suzen, Y.B., Huang, P.G., 2001. Predictions of separated and transitional boundary layers under low pressure turbine airfoil conditions using an intermittency transport equation. AIAA 200-0446, 39th AIAA Aerospace Sciences Meeting and Exhibit, Reno, Nevada, January 8–11.

Wilcox, D.C., 1993. Turbulence Modeling for CFD. DCW Industries, Inc.